Materials Advances

ROYAL SOCIETY OF CHEMISTRY

COMMUNICATION

View Article Online
View Journal | View Issue

Check for updates

Cite this: *Mater. Adv.*, 2022, 3, 8137

Received 20th June 2022,
Accepted 22nd August 2022

DOI: 10.1039/d2ma00713d

rsc.li/materials-advances

Large-scale production of Au nanoparticles as medical antibiotics†

Hongyu Meng, ‡[a] Shiyu Cheng,‡[b] Le Wang,[b] Yekkuni L. Balachandran,[b] Wei Zhang*[b] and Xingyu Jiang *[b]

Here we present a process of producing AuNPs on a large scale upon further development of the bench scale experiment. We produce an AuNP-based medical dressing by using dyeing and finishing machines. The AuNPs and related products are very promising in medical applications.

Gold nanoparticles (AuNPs) are regarded as a kind of biocompatible material, which is chemically stable, easily modifiable with certain chemicals, and non-toxic to mammalian cells.[1] Some drugs containing AuNPs have been approved by the US FDA to treat cancer.[1] Antibiotics conjugated to AuNPs show remarkably enhanced antibacterial activity compared with antibiotics alone, although AuNPs alone without modified antibiotics have no activity against these strains.[2–4] In recent years, we have devoted our attention to the development of safe and effective AuNP antibacterial agents.[5–12] We found that AuNPs modified by small non-antibiotic drugs (DAPT and DMB) have excellent antibacterial effect on Gram-negative bacteria, such as *Escherichia coli* (*E. coli*) and *Pseudomonas aeruginosa* (*P. aeruginosa* or *P. a*), and Gram-positive bacteria, such as *Staphylococcus aureus* (*S. aureus* or *S. a*), but exhibited no bacterial resistance.[6] Meanwhile, the cytotoxicity of the AuNPs is much less than that of AgNPs.[13–18] AuNPs and AuNP-based antibacterial agents modified with non-antibiotics drugs are thus very promising in clinical applications. Our previous work mainly focused on preparing antibacterial AuNPs on a bench scale, and their medical use has been largely limited due to the difficulty in large-scale production.[19,20]

Here, we introduce a method of producing the AuNPs on a large scale and a process of manufacturing an AuNP-based medical dressing by using continuous dyeing and finishing machines. We confirmed the effectiveness of this method by testing the influence of dialysis, speed of adding $NaBH_4$, and different production scales on the antibacterial ability of AuNPs and by comparing with commercial antibacterial AgNPs. This approach is very straightforward, low-cost, and suitable for large scale production.

We investigated the antibacterial ability of AuNPs (before and after dialysis) and each component. In our previous work, we have reported that the antibacterial AuNPs should be purified by dialysis (Mw = 14 kDa) in deionized water for more than 24 h before use.[5,6] However, this is unpractical for the industrial-scale production of AuNPs due to its high cost and complex procedures. By using the microbroth dilution method according to the National Committee for Clinical Laboratory Standards M7-A8 (2009), we determined the minimum inhibitory concentration (MIC) of AuNPs with and without dialysis. We can clearly see that the antibacterial ability of AuNPs without dialysis is much better than that of AuNPs after dialysis (Table 1), but the cytotoxicity of the two AuNPs is similar, much less than that of AgNPs and $AgNO_3$ (Fig. 3). We also tested the antibacterial activity of each component used in preparing AuNPs (Table 1). Tween 80, $NaBH_4$, 4,6-diamino-2-pyrimidinethiol (DAPT) and 1,1-dimethylbiguanide (DMB) below the synthesized concentration showed no effective antibacterial activity to the three kinds of bacteria. Acetic acid showed some antibacterial activity, but much less than AuNPs. We can infer that dialysis will reduce the antibacterial effect of the AuNPs to some extent. Thus,

Table 1 Antibacterial activities of components in preparing AuNPs

MIC (mg L^{-1})	*E. coli*	*S. aureus*	*P. aeruginosa*
Acetic acid	4200	4200	4200
Tween 80	>2592	>2592	>2592
$NaBH_4$	>456	>456	>456
DAPT	>568	>568	>568
DMB	>660	>660	>660
$HAuCl_4{\cdot}3H_2O$	40	80	160
AuNPs (without dialysis)	3	6	6
AuNPs (after dialysis)	10	40	80

[a] *CAS Center for Excellence in Nanoscience, Beijing Key Laboratory of Micro-Nano Energy and Sensor, Beijing Institute of Nanoenergy and Nanosystems, Chinese Academy of Sciences, Beijing, 101400, China*

[b] *Department of Biomedical Engineering, Southern University of Science and Technology, Shenzhen, Guangdong 518055, China. E-mail: jiang@sustech.edu.cn*

† Electronic supplementary information (ESI) available. See DOI: https://doi.org/10.1039/d2ma00713d

‡ These authors contributed equally to this work.

Open Access Article. Published on 14 October 2022. Downloaded on 2/20/2026 5:09:43 AM. This article is licensed under a Creative Commons Attribution-NonCommercial 3.0 Unported Licence.

Open Access Article. Published on 14 October 2022. Downloaded on 2/20/2026 5:09:43 AM.
This article is licensed under a Creative Commons Attribution-NonCommercial 3.0 Unported Licence.

the dialysis process is not needed for their large-scale production and potential medical applications.

We added the AuNPs or other reagents at a gradually halving concentration in the MH broth in a 96-well microplate and added the same amount of bacterial suspension in all the microwells. So each well in the row of the 96-well microplate had a decreasing amount of the reagent but the same amount of bacteria before incubation. After incubation, for a reagent, a higher number of microwells with non-visible bacterial growth indicates a smaller MIC and better antibacterial ability (details are shown in the ESI†).

We tested the relationship between the time of $NaBH_4$ addition and the properties of AuNPs. In our previous work, we added an aqueous solution of $NaBH_4$ (the reductant) to the reaction solution dropwise. In this way, the time of $NaBH_4$ addition is 20 min at a 250 mL scale and 13 h at a 10 L scale.[5,6] We speed up the addition of $NaBH_4$, which has largely reduced the time of $NaBH_4$ addition. At a 250 mL scale, we added $NaBH_4$ solution into the reaction solution at different speeds, which took 10 s, 5 min, 10 min, and 20 min, respectively. The UV-Vis spectra of AuNPs showed that the concentration of AuNPs had little change (Fig. 1C). The average size of AuNPs decreased slightly with the decrease of the speed of the addition of $NaBH_4$ solution, in the order of 5.5 ± 1.4 nm, 4.2 ± 0.9 nm, 3.5 ± 1.1 nm, and 3.1 ± 0.8 nm (Fig. 1A and B). According to the analysis, the slower addition of $NaBH_4$ promoted the interaction of $HAuCl_4$ and $NaBH_4$, thereby making the AuNPs smaller and their distribution more uniform. However, the antibacterial ability of AuNPs of the 250 mL batch has little change at different times of $NaBH_4$ addition (Fig. 1D), similar to that of the bench scale.

To evaluate the influence of different scales of production on the properties of AuNPs, we prepared the AuNPs (without dialysis) starting from different volumes of solution, including 25 mL, 250 mL, 5 L and 10 L. The NaBH4 solution was added to the reaction solution at an increased speed. The duration of addition of 25 mL and 250 mL scales is less than 10 seconds. The duration of the 5 L scale is about 1 min and the duration of the 10 L scale is about 2 min. The speed of stirring is decreased as the volume of the solution increases (Table 2). The size distribution of AuNPs prepared at 25 mL and 250 mL scales was 4.4 ± 0.7 nm and 3.9 ± 1.2 nm. When the scale reaches 5 L and 10 L, the size of AuNPs was 2.7 ± 0.5 nm and 2.5 ± 0.3 nm (Fig. 2A and B). We suspected that a relatively large reaction scale promoted the dispersion of $NaBH_4$ and interaction between reactants, and thus AuNPs exhibited a smaller diameter and a more uniform distribution. Moreover, the concentration and the MIC of AuNPs produced at litre and milliliter scales had small variations (Fig. 2C and D). We realized the large scale production of the antibacterial AuNPs. By using 10 L AuNPs, we could fabricate antibacterial medical dressings with an area of 650–850 m^2, which could meet the needs of 650–850 patients with wounds.

Table 2 Stirring speed at different volumes

Volume	Speed of stirring (rpm)
25 mL	800
250 mL	800
5 L	100
10 L	70

We compared AuNPs with the commercially available AgNPs (Changsha Hairun Co. Ltd, China). AuNPs and AgNPs (Fig. S1, ESI†) are both spherical and their sizes are similar. For *E. coli*, the MIC of AuNPs is about 1.5 mg L^{-1}, which is lower than that of AgNPs (about 3.5 mg L^{-1}) (Fig. 2D). The MIC of AuNPs to *S. a* is about 5.8 mg L^{-1} and the MIC of AgNPs to *S. a* is below 4 mg L^{-1}. The MICs of AuNPs and AgNPs to *P. a* are both about 4 mg L^{-1}.

AuNPs display better performance than AgNPs in medical antibacterial applications, especially in terms of toxicity to human cells. We performed the cytotoxicity test with HUVEC cells. The toxicity of AuNPs is far less than that of AgNPs and $AgNO_3$ (Fig. 3C). At a 50 mg L^{-1} concentration of antibacterial agents, the cell viability of AuNPs is above 80%, while the cell viability of AgNPs and $AgNO_3$ is below 50%.

We prepared an AuNP-based gauze on a bench scale and large scale by using continuous dyeing and finishing machines.

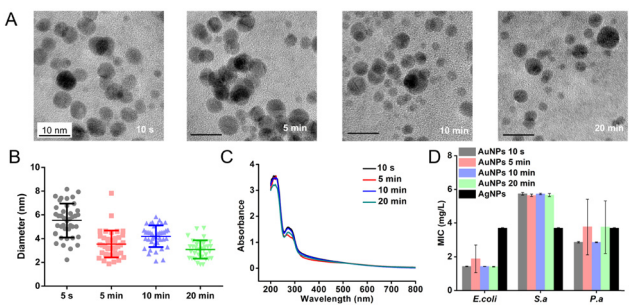

Fig. 1 Effects of different speeds of $NaBH_4$ addition on the properties of AuNPs. (A) TEM images of AuNPs synthesized with different speeds of $NaBH_4$ addition. (B) Size distribution of AuNPs synthesized with different speeds of $NaBH_4$ addition. Data are shown as mean ± standard deviation (n = 40). (C) UV-Vis spectra of AuNPs. (D) Antibacterial activities of AuNPs and commercial AgNPs against *E. coli*, *S. a* and *P. a* indicated by MIC (μg mL^{-1}).

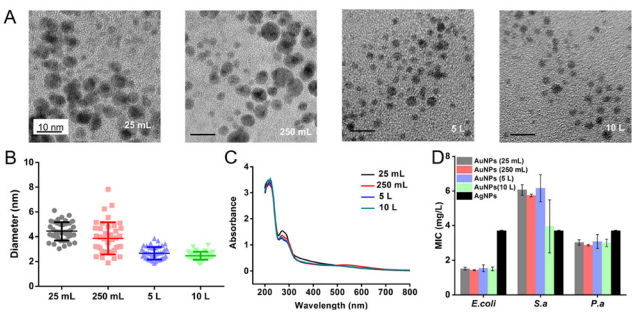

Fig. 2 Effect of different scales on the properties of AuNPs. (A) TEM images of AuNPs synthesized at different synthesis scales. (B) Particle size distribution of AuNPs synthesized at different synthesis scales. Data are shown as mean ± standard deviation (n = 40). (C) UV-Vis spectra of AuNPs synthesized at different synthesis scales. (D) Antibacterial activities of AuNPs and the commercial AgNPs against *E. coli*, *S. a* and *P. a* indicated by MIC (μg mL^{-1}).

© 2022 The Author(s). Published by the Royal Society of Chemistry

Open Access Article. Published on 14 October 2022. Downloaded on 2/20/2026 5:09:43 AM.
This article is licensed under a Creative Commons Attribution-NonCommercial 3.0 Unported Licence.

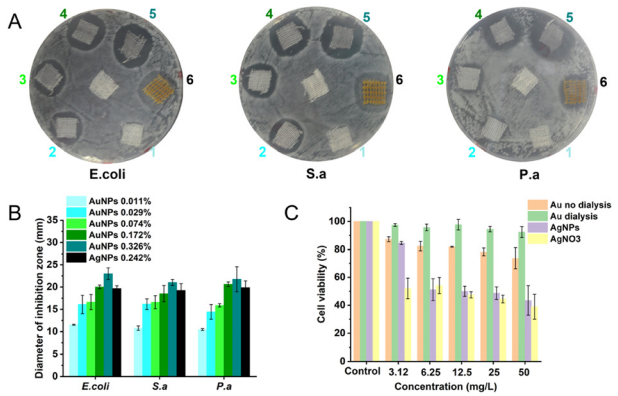

Fig. 3 The comparison between AuNPs and AgNPs in terms of antibacterial activity and cytotoxicity. (A) Photographs of the inhibition zone of the AuNP-based gauze with different AuNP contents. No. 6 is the commercially available AgNP-based gauze, and the gauze without a reagent at the center of the plate is the control. (B) Diameter of the inhibition zone of the AuNP-based gauze with different AuNP contents. (C) Cytotoxicity of AuNPs without dialysis, AuNPs after dialysis, commercially available AgNPs and $AgNO_3$ at different concentrations.

We evaluated the antibacterial activity of the AuNP-based gauze and a commercially available AgNP-based gauze against *E. coli, S. aureus*, and *P. aeruginosa*.[10] We spread 0.5 mL of each bacterial suspension on a nutrient agar plate in a sterilized Petri dish. We placed gauzes with different AuNP contents on an agar plate and incubated them at 37 °C for 24 h before observation (Fig. 3). The mass content of AuNPs in the gauze is 0.011%, 0.029%, 0.074%, 0.172% and 0.326% for No. 1 to No. 5, respectively. No. 6 is the commercially available AgNP-based gauze and the mass content of AgNPs in the gauze is 0.242%. The AuNP-based gauze had a good antibacterial effect as the commercial product (Changsha Hairun Co. Ltd, China) containing a similar mass percentage of AgNPs.

We prepared the AuNP-based gauze at a bench scale and large scale. The color of the AuNP-based gauze is beige (Fig. 4A) and the color of the AgNP-based gauze is brown (Fig. 4D).

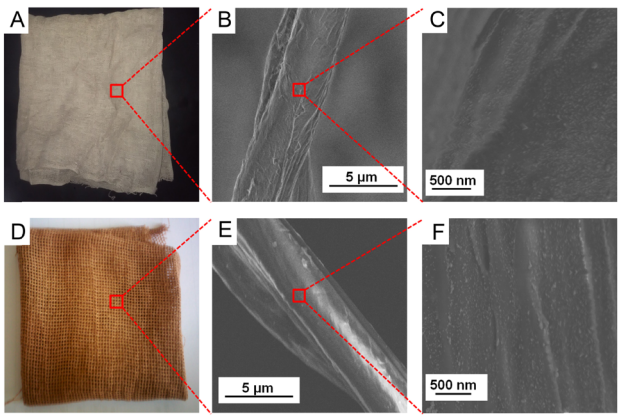

Fig. 4 Images of the AuNP-based gauze and commercial AgNP-based gauze. (A) Image of the AuNP-based gauze. (B and C) SEM images of the AuNP-based gauze. (D) Image of the commercial AgNP-based gauze. (E and F) SEM images of the commercial AgNP-based gauze.

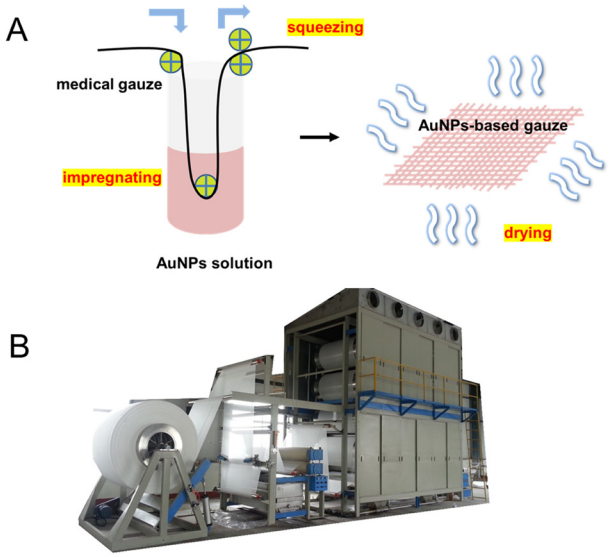

Fig. 5 Mass production of the AuNP-based gauze. (A) Flow diagram of producing the AuNP-based gauze through impregnation, squeezing and drying. (B) Using continuous dyeing and finishing machines to produce the AuNP-based gauze.

The mass content of AuNPs in the gauze ranges from 0.011% to 0.326%. The AuNPs and AgNPs were distributed on the surface of the fibers of the gauze (Fig. 4). At the bench scale, the gauze was immersed into the AuNP solution and the concentration of the AuNP solution can be adjusted. We squeezed the gauze to remove the excess solution with a lab padder. The gauze was dried in a dryer at 150 °C for 10 min. The drying temperature should be higher than the boiling point of acetic acid (118 °C) to remove acetic acid. This temperature does not affect the structure of the gauze or AuNPs. We conducted the mass production by using continuous dyeing and finishing machines (Fig. 5B).

Conclusions

In this paper, we present the large-scale production of antibacterial AuNPs *via* adjusting the process of adding $NaBH_4$ with the elimination of dialysis. We produce an AuNP-based medical gauze on a large scale through impregnation, squeezing and drying by using continuous dyeing and finishing machines, and the production method is suitable for other water-soluble nanoparticles. The AuNPs and their related medical products are very promising in clinical applications.

Author contributions

Honyu Meng: conceptualization, methodology, investigation, formal analysis, writing – original draft. Shiyu Chen: methodology, visualization, writing – review & editing. Le Wang: methodology, formal analysis. Yekkuni L. Balachandran: formal analysis, software, validation. Wei Zhang: conceptualization, methodology, formal analysis, project administration. Xingyu Jiang:

methodology, resources, funding acquisition, project administration, writing – review & editing.

Conflicts of interest

There are no conflicts to declare.

Acknowledgements

We thank Shenzhen Science and Technology Program (KQTD20190929172743294), the National Natural Science Foundation of China (21535001, 81730051, and 81673039), the National Key R&D Program of China (2018YFA0902600), the Chinese Academy of Sciences (QYZDJ-SSW-SLH039 and 121D11KYSB20170026), Shenzhen Bay Laboratory (SZBL2019062801004), and Tencent Foundation through the XPLORER PRIZE for financial support.

Notes and references

1 M. A. Dobrovolskaia, D. R. Germoler and J. L. Weaver, *Nat. Nanotechnol.*, 2009, **4**, 411–414.
2 H. Lai, W. Chen, C. Wu and Y. Chen, *ACS Appl. Mater. Interfaces*, 2015, **7**, 2046–2054.
3 H. Gu, P. L. Ho, E. Tong, L. Wang and B. Xu, *Nano Lett.*, 2013, **3**, 1261–1263.
4 Y. Zhao and X. Jiang, *Nanoscale*, 2013, **5**, 8340–8350.
5 Y. Zhao, Y. Tian, Y. Cui, W. Ma and X. Jiang, *J. Am. Chem. Soc.*, 2010, **132**, 12349–12356.
6 Y. Zhao, Z. Chen, Y. Chen, J. Xu, J. Li and X. Jiang, *J. Am. Chem. Soc.*, 2013, **135**, 12940–12943.
7 Y. Cui, Y. Zhao, Y. Tian, W. Zhang and X. Jiang, *Biomaterials*, 2012, **33**, 2327–2333.
8 Y. Zhao, C. Ye, W. Liu, R. Chen and X. Jiang, *Angew. Chem., Int. Ed.*, 2014, **53**, 8127–8131.
9 Y. Xie, Y. Liu, J. Yang, Y. Liu, F. Hu and X. Jiang, *Angew. Chem., Int. Ed.*, 2018, **57**, 3958–3962.
10 X. Yang, Q. Wei, H. Shao and X. Jiang, *ACS Appl. Mater. Interfaces*, 2019, **11**, 7725–7730.
11 L. Wang, S. Li, J. Yin, J. Yang, Q. Li, W. Zheng, S. Liu and X. Jiang, *Nano Lett.*, 2020, **20**, 5036–5042.
12 X. Zhao, Y. Jia, R. Dong, J. Deng, H. Tang, F. Hu, S. Liu and X. Jiang, *Chem. Commun.*, 2020, **56**, 10918–10921.
13 S. Eckhardt, P. S. Brunetto, J. Gagnon, M. Priebe, B. Giese and K. M. Fromm, *Chem. Rev.*, 2013, **113**, 4708–4754.
14 X. Chen and H. J. Schluesener, *Toxicol. Lett.*, 2008, **176**, 1–12.
15 I. Chopra, *J. Antimicrob. Chemother.*, 2007, **59**, 587–590.
16 K. Kawata, M. Osawa and S. Okabe, *Environ. Sci. Technol.*, 2009, **43**, 6046–6051.
17 M. Ema, H. Okuda, M. Gamo and K. Honda, *Reprod. Toxicol.*, 2017, **67**, 149–164.
18 L. Wang, W. Zheng and X. Jiang, *Chem. Commun.*, 2020, **56**, 6664–6667.
19 N. Du, H. Wu, H. Zhang, C. Zhai, P. Wu, L. Wang and D. Yang, *Chem. Commun.*, 2011, **47**, 1006–1008.
20 C.-T. Dinh, T.-D. Nguyen, F. Kleitz and T.-O. Do, *Chem. Commun.*, 2011, **47**, 7797–7799.

Open Access Article. Published on 14 October 2022. Downloaded on 2/20/2026 5:09:43 AM.
This article is licensed under a Creative Commons Attribution-NonCommercial 3.0 Unported Licence.

© 2022 The Author(s). Published by the Royal Society of Chemistry